Combining QCD matrix elements at next-to-leading order with parton showers in electroproduction

Björn Pötter
Max-Planck-Institut für Physik, Werner-Heisenberg-Institut, Föhringer Ring 6, 80805 Munich, Germany
(Received 26 July 2000; revised manuscript received 9 February 2001; published 3 May 2001)

We present a method to combine next-to-leading order (NLO) matrix elements in QCD with leading logarithmic parton showers by applying a suitably modified version of the phase-space-slicing method. The method consists of subsuming the NLO corrections into a scale-dependent phase-space-slicing parameter, which is then automatically adjusted to cut out the leading order, virtual, soft and collinear contributions in the matrix element calculation. In this way a positive NLO weight is obtained, which can be redistributed by a parton shower algorithm. As an example, we display the method for single-jet inclusive cross sections at $\mathcal{O}(\alpha_s)$ in electroproduction. We numerically compare the modified version of the phase-space-slicing method with the standard approach and find very good agreement on the percent level.

DOI: 10.1103/PhysRevD.63.114017 PACS number(s): 13.85.Hd, 13.65.+i

I. INTRODUCTION

Much progress has been made in the last years in measuring the hadronic final state in eP scattering at the DESY eP collider HERA with high precision (see [1] for a recent review). The theoretical tools which are at hand to describe the hadronic final state are basically fixed order perturbative calculations, which for most processes are available at next-to-leading order (NLO), or a combination of leading order (LO) matrix elements with parton showers (PS's), mostly at leading logarithmic accuracy, which are implemented in event generators (see [2] for an overview of available Monte Carlo programs for both approaches). However, it appears that the theoretical calculations are a considerable source for errors in determining physical parameters. As an example, the statistical errors in a recent determination of α_s from dijet production [3] are at the 1% level. The systematical and theoretical errors, on the other hand, are considerably larger and both lie around 5%. Therefore, an improvement of the theoretical tools is needed.

The fixed higher order and the PS approaches have complimentary strengths. The fixed higher order calculations reduce uncertainties due to unphysical renormalization and factorization scale dependences. Wide-angle emission of partons, where interference effects between a large number of diagrams may be important, is described well. The PS on the other hand allows a description of the cross section in regions where α_s becomes large, especially in the region of collinear particle emission, by means of a resummation of large logarithmic terms. This allows us to, e.g., describe reasonably well the substructure of jets. In addition, the PS can be terminated at some small scale Q_0, which allows us to attach some kind of hadronization model, as, e.g., the Lund model [4], to describe the nonperturbative region. It is desirable to find a way of combining the advantages of both approaches into a NLO event generator. In a complete NLO event generator one certainly would like to include not only the matrix elements at NLO, but likewise the PS in next-to-leading log accuracy. Two problems in combining parton showers and matrix elements can be identified. First, one has to avoid double counting of events which are included both in the matrix element calculations and in the PS. Second, negative weights can occur in the calculation of the matrix elements at NLO. Although they are not a principle problem, negative weights can make it difficult in practice to obtain numerically stable results when they are used as a starting point for the PS.

Basically two strategies can be adopted to combine matrix elements and PS's. Either the phase space is split into two parts, using the matrix element cross sections in one region and the PS in the other [5–7], or the PS algorithm is modified as to reproduce the matrix element cross section in the hard limit [8]. In current event generators such as, e.g., PYTHIA [9] or HERWIG [10], leading log parton showers are combined with leading order matrix elements in the wide angle scattering region. Recently attempts were made to improve the leading order accuracy in these approaches by going to next-to-leading order. In [11] both, the PS and the matrix elements were modified to obtain a smooth merge of the PS to the higher order calculation. Collins [12] suggested a procedure to subtract from the matrix elements those parts which are included already in the PS. Since the PS describes the soft and collinear region, the divergences associated with the matrix element calculation in this region are avoided. Finally, Sjöstrand and Friberg [13] suggested an improvement of the splitting procedure, by using the NLO matrix elements to calculate the weight for the PS region instead of the LO weight. They suggested introducing a function which approximates the weight in the PS region in such a way that the negative weight problem is largely avoided. However, Sjöstrand and Friberg only gave an outline of their method without providing the approximate function for any specific process, and hence they also did not give numerical results.

In this paper, we take the suggestions in [13] as a starting point and give further details for a general method to get the correct NLO normalization of the PS region. To avoid negative weights, we rely on an older suggestion by Baer and Reno [14], based on the phase-space-slicing method. Baer and Reno suggested introducing a phenomenologically determined fixed slicing parameter such that the sum of the Born, virtual, soft, and collinear contributions is approximately

zero. In this paper, we *calculate* a scale dependent cutoff function, which provides a cutoff for each phase-space point, such that the sum is *exactly* zero and the improved scale and scheme dependence of the NLO calculations is preserved. The NLO corrections are given by the NLO hard tree-level matrix elements integrated down to the cutoff. Since these contributions are positive definite, the NLO weight obtained from this method can be directly redistributed according to a PS algorithm.

The paper consists of two main parts. In the first part we discuss the general method to combine matrix elements at NLO with PS's by use of the described cutoff function. In the second part we consider as a physically important and interesting example single-jet production in deep inelastic scattering (DIS). Here, the LO contribution is of order α_s^0 and the NLO corrections are of order α_s. Including higher order matrix elements for this process will become especially important for diffractive DIS, since the gluon density in the proton at small x_{bj} is large compared to the quark density. Therefore, the photon-gluon fusion process, which is a NLO correction to the first order quark-parton model contribution, will not necessarily be small. We explicitly construct and numerically study the cutoff function for this case. Finally, we summarize our results and give an outlook for future developments.

II. GENERAL METHOD

A. Jet cross sections at next-to-leading order

We start by summarizing the procedure for the numerical evaluation of an inclusive n-jet cross section in NLO QCD. The first step is to select a jet algorithm, which defines how partons are recombined to give jets. In the following we take for definiteness the invariant mass s_{ij} of two partons i and j and define the n-jet region such that $s_{ij}<s_{\min}$, with some kind of minimum mass $s_{\min}$ and likewise the $(n+1)$-jet region such that $s_{ij}>s_{\min}$ for all i,j. The LO process for the production of n jets consists of n final state partons and obviously does not depend on the jet definition. This dependence only comes in at NLO. The $\mathcal{O}(\alpha_s)$ corrections to this process are given by the ultraviolet (UV) and infrared (IR) divergent one-loop contributions to the n-parton configuration, which are the virtual corrections, and the NLO tree level matrix elements with $(n+1)$ partons, the real corrections. The tree-level matrix elements have to be integrated over the phase space of the additional parton, which gives rise to collinear and soft singularities. After renormalization, the singularities in the virtual and soft or collinear contributions cancel and remaining poles are absorbed into parton distribution functions. One wants to integrate most of the phase space of the real corrections numerically, but one needs to find a procedure to calculate the soft or collinear contributions analytically as to explicitly cancel the poles from the virtual corrections. The two basic methods to perform these integrations are the subtraction method [15–17] and the phase-space-slicing (PSS) method [18–21] (see also [22] for a review).

In the following we will make use of the PSS method and therefore discuss this method further. To illustrate the method, we rely on the classical example given by Kunszt and Soper [16]. We label the LO Born contribution as $\sigma^{\mathrm{LO}}=\sigma^B$. The NLO cross section is given by the sum of the Born cross section and the virtual and real corrections, σ^V and σ^R,

$$\sigma^{\mathrm{NLO}}=\sigma^B+\sigma^V+\sigma^R=\sigma^B+C_V-\lim_{\epsilon\to 0}\frac{1}{\epsilon}F(0)+\int_0^1\frac{dx}{x}F(x). \tag{1}$$

Here, $F(x)$ is the known, but complicated function representing the $(n+1)$-parton matrix elements. The variable x represents an angle between two partons or the energy of a gluon, the integral represents the phase-space integration that has to be performed over the additional parton. The singularity of the real corrections at $x\to 0$ is compensated by the virtual corrections, given by the pole term and some constant, C_V. In the PSS method, the integral over the real corrections is divided into two parts, $0<x<\delta$ and $\delta<x<1$. We note that the technical cutoff δ should lie within the n jet region, i.e., if we define $y_{\mathrm{cut}}=s_{\min}/Q^2$, then we should have $\delta<y_{\mathrm{cut}}$. If the cutoff parameter is sufficiently small, $\delta\ll y_{\mathrm{cut}}<1$, one can write

$$\begin{aligned}\sigma^R&=\int_0^1\frac{dx}{x}F(x)\simeq\lim_{\epsilon\to 0}\left\{\int_\delta^1\frac{dx}{x}x^\epsilon F(x)+F(0)\int_0^\delta\frac{dx}{x}x^\epsilon\right\}\\&\simeq\int_\delta^1\frac{dx}{x}F(x)+F(0)\ln(\delta)+\lim_{\epsilon\to 0}\frac{1}{\epsilon}F(0),\end{aligned} \tag{2}$$

where the integral has been regularized by the term x^ϵ, as suggested by dimensional regularization. The pole is now explicit and the NLO cross section σ^{NLO} is finite:

$$\sigma^{\mathrm{NLO}}\simeq\sigma^B+C_V+\int_\delta^1\frac{dx}{x}F(x)+F(0)\ln(\delta). \tag{3}$$

Clearly, the real corrections σ^R should not depend on δ, and the logarithmic δ dependence of the last term in Eq. (3) should be canceled by the integral, which sometimes is numerically difficult for very small parameters δ. However, an improvement of the above solution is possible by using a hybrid of the PSS and the subtraction methods suggested by Glover and Sutton [23]. In this method, one adds and subtracts only the universal soft/collinear approximations for $x<\delta$, such that

$$\begin{aligned}\sigma^R&=\lim_{\epsilon\to 0}\left\{\int_0^1\frac{dx}{x}x^\epsilon F(x)-F(0)\int_0^\delta\frac{dx}{x}x^\epsilon+F(0)\int_0^\delta\frac{dx}{x}x^\epsilon\right\}\\&\simeq\int_\delta^1\frac{dx}{x}F(x)+\int_0^\delta\frac{dx}{x}[F(x)-F(0)]+F(0)\ln(\delta)\\&\quad+\lim_{\epsilon\to 0}\frac{1}{\epsilon}F(0).\end{aligned} \tag{4}$$

A cancellation between the analytical and numerical terms still occurs; however, only the phase space is approximated,

so that this method is valid at larger values of δ. In the case where the phase space is not approximated for small x the hybrid method becomes independent from δ.

B. Event generation with positive NLO weights

We would now like to improve the above NLO jet cross section by including the PS in the n-jet region. We keep the jet definition, which separates the available phase space into two complementary regions, namely, the n-jet region for $s_{ij} < s_{\min}$ and the $(n+1)$-jet (hard) region for $s_{ij} > s_{\min}$. The NLO corrections, i.e., the virtual and the soft or collinear corrections, will occur in the n-jet region, so that the n-jet exclusive cross section has a NLO normalization. On the other hand, the hard $(n+1)$-jet region contains tree-level contributions only.

In current event generators, a weight will be generated in the n-jet region by calculating the LO, tree-level matrix element and then redistributing this weight with help of the PS algorithm. The same jet criterion used to separate the matrix element and PS regions is used to veto events from the PS which would lie outside the n-jet region, as to avoid double counting. The $(n+1)$-jet region is described by the hard $(n+1)$-parton matrix elements.

If we take the procedure for calculating the NLO corrections as described in the previous section, we could in principle calculate the weight in the n-jet region in NLO. However, we would like to avoid the generation of large positive and negative weights, since this is not a practical starting point for an event generator, especially if one wishes to add hadronization after the showering. Therefore we suggest to choose the PSS parameter δ such that the weights are always positive. To keep the advantages of the NLO calculation, we aim to find a cutoff function $\delta^{\rm nlo}(\mu^2)$ that provides a cutoff parameter for any given renormalization and factorization scale which lies inside the n-jet region, such that the sum of the Born, soft or collinear and virtual contributions are exactly zero. The NLO corrections inside the jet are then completely enclosed in the $(n+1)$-parton hard matrix elements, integrated down to the cutoff function. Only the tree-level matrix elements will serve as starting points for the PS. The reduced scale and scheme dependence of the NLO cross sections is subsumed into the scale dependent cutoff function. Staying in the simple example from Eq. (1), the aimed cutoff function reads

$$\delta^{\rm nlo} = \exp\left(-\frac{\sigma^B}{F(0)} - \frac{C_V}{F(0)} \right). \tag{5}$$

Substituting δ in Eq. (3) by $\delta^{\rm nlo}$ results in

$$\sigma^{\rm NLO} \simeq \int_{\delta^{\rm nlo}}^1 \frac{dx}{x} F(x), \tag{6}$$

which is exactly what we are looking for. The NLO corrections are given completely by the hard $(n+1)$-parton tree-level matrix elements, which are positive definite and can be combined with the PS in the usual way. The function $\delta^{\rm nlo}$ will depend on the kinematics of the n parton configuration, as well as on the renormalization and factorization scales. Of course, one has to ensure in the event generation process that $\delta^{\rm nlo} < y_{\rm cut}$, i.e., that the cutoff lies within the n-jet region.

In general, the function (5) could yield a relatively large δ, so that the simple PSS method fails to give the correct answer for the NLO cross section.[1] We can, however, calculate the missing parts of the approximated matrix elements, which is the cause of the error, numerically by use of the hybrid method described above. Improving the result (6) with the hybrid method, one finds

$$\sigma^{\rm NLO} \simeq \int_{\delta^{\rm nlo}}^1 \frac{dx}{x} F(x) + \int_0^{\delta^{\rm nlo}} \frac{dx}{x} [F(x) - F(0)], \tag{7}$$

which gives additional terms of order $\delta^{\rm nlo} \ln(\delta^{\rm nlo})$. Here, the difference between the approximate function $F(x)|_{x=0}$ and the full expression is evaluated numerically. This is similar to what Sjöstrand and Friberg suggested in [13] as a starting point for the event generation.

To summarize, we propose in close analogy to [13] the following steps to produce an event in the PS region with positive weight and NLO normalization:

(1) Define the n-jet region by

$$s_{ij} < y_{\rm cut} Q^2 \tag{8}$$

for all partons i,j. The $(n+1)$-jet region given by $s_{ij} > y_{\rm cut}$ is described by the hard $(n+1)$-parton matrix elements.

(2) For each n-jet phase-space point calculate $\delta^{\rm nlo}$ according to Eq. (5). The cross section for the n-jet region is then given by

$$\begin{aligned} \sigma^{\rm NLO}_{n\text{-}jet} &= \sigma^B + \sigma^V + \sigma^R \\ &= \int_{\delta^{\rm nlo}}^{y_{\rm cut}} \frac{dx}{x} F(x) + \int_0^{\delta^{\rm nlo}} \frac{dx}{x} [F(x) - F(0)]. \end{aligned} \tag{9}$$

We can write this symbolically as

$$\sigma^{\rm NLO}_{n\text{-}jet} = (y_{\rm cut} - \delta^{\rm nlo}) \left\langle \frac{F(x)}{x} \right\rangle + \delta^{\rm nlo} \left\langle \frac{F(x) - F(0)}{x} \right\rangle \tag{10}$$

so as to express the Monte Carlo nature of the procedure.

(3) In the n-jet region generate an $x_k = s_{ij}^k / Q^2$ with $x_k \in [0, y_{\rm cut}]$ (the index k refers to the kth event). The weight which will be redistributed by the parton shower algorithm is given by

$$W_k = (y_{\rm cut} - \delta^{\rm nlo}) \left\langle \frac{F(x)}{x} \right\rangle \Bigg|_{x = x_k}$$

for $x_k \in [\delta^{\rm nlo}, y_{\rm cut}]$, where $W > 0$ by construction, or by

$$W_k = \delta^{\rm nlo} \left\langle \frac{F(x) - F(0)}{x} \right\rangle \Bigg|_{x = x_k}$$

[1] As we will see in the second part of the paper, for DIS single-jet production at $\mathcal{O}(\alpha_s)$ the cutoff $\delta^{\rm nlo}$ actually is sufficiently small for the soft and collinear approximations to be valid.

for $x_k \in [0,\delta^{\rm nlo}]$, where W will be rather small.

(4) Use the same jet resolution criterion as in the first step to veto events from the PS that lie within the $(n+1)$-jet region.

III. INCLUSIVE SINGLE-JET PRODUCTION IN DIS

In the following we apply the ideas of the previous section to inclusive single-jet production in DIS eP scattering at $\mathcal{O}(\alpha_s)$. For this, we recall the formulas for calculating single-jet cross sections at NLO with the standard PSS method and describe the modified version of the PSS method, which is used to evaluate the cutoff function. We numerically compare the modified with the standard method.

A. Single-jet cross section up to $\mathcal{O}(\alpha_s)$

In eP scattering

$$e(k)+P(p)\to e(k')+X \tag{11}$$

the final state with a single jet is the most basic event with a large transverse energy E_T in the laboratory frame. The lowest order $\mathcal{O}(\alpha_s^0)$ partonic contribution to the single-jet cross section arises from the quark parton model (QPM) subprocess

$$e(k)+q(p_0)\to e(k')+q(p_1) \tag{12}$$

and the corresponding antiquark process with $q\leftrightarrow\bar{q}$. The partonic cross section for this process is given by

$$\hat{\sigma}^{\rm LO}_{q\to q}=\sigma_0 e_q^2 |M_{q\to q}|^2 \tag{13}$$

where

$$\sigma_0=\frac{1}{4p_0\cdot k}\frac{1}{4}\frac{(4\pi\alpha)^2}{Q^4} \tag{14}$$

and

$$|M_{q\to q}|^2=32[(p_0\cdot k)^2+(p_0\cdot k')^2]=8\hat{s}^2[1+(1-y)^2]. \tag{15}$$

Here, $\hat{s}=xs$, with $s=(k+p)^2$, denotes the partonic center of mass energy squared, α is the electromagnetic coupling, and $Q^2=2(k\cdot k')$ is the photon virtuality. The total DIS cross section can be directly obtained by integrating out the complete phase space of the final state parton.

At NLO, the single-jet cross section receives contributions from the real and the one-loop virtual corrections. The real corrections consist of the photon-gluon fusion and the QCD-Compton processes

$$e(k)+q(p_0)\to e(k')+q(p_1)+g(p_2), \tag{16}$$

$$e(k)+g(p_0)\to e(k')+q(p_1)+\bar{q}(p_2), \tag{17}$$

together with corresponding antiquark processes. The partonic cross sections for one-photon exchange are

$$\alpha_s\hat{\sigma}^{\rm LO}_{q\to qg}=\sigma_0 e_q^2[4\pi\alpha_s(\mu_R)]|M_{q\to qg}|^2, \tag{18}$$

$$\alpha_s\hat{\sigma}^{\rm LO}_{g\to q\bar{q}}=\sigma_0 e_q^2[4\pi\alpha_s(\mu_R)]|M_{g\to q\bar{q}}|^2, \tag{19}$$

with

$$|M_{q\to qg}|^2=\frac{128}{3}(k\cdot k')\times\frac{(k\cdot p_0)^2+(k'\cdot p_0)^2+(k\cdot p_1)^2+(k'\cdot p_1)^2}{(p_1\cdot p_2)(p_0\cdot p_2)}, \tag{20}$$

$$|M_{g\to q\bar{q}}|^2=-\frac{3}{8}|M_{q\to qg}|^2(p_0\leftrightarrow -p_2)=16(k\cdot k')\times\frac{(k\cdot p_2)^2+(k'\cdot p_2)^2+(k\cdot p_1)^2+(k'\cdot p_1)^2}{(p_0\cdot p_1)(p_0\cdot p_2)}. \tag{21}$$

Color factors (including the initial state color average) are included in the squared matrix elements. Note that the initial state spin average factors are included in the definition of σ_0 in Eq. (15) and that the results in Eqs. (20),(21) contain the full polarization dependence of the virtual boson.

As already discussed in the previous section, the real corrections inherit characteristic divergencies, which are the initial and final state soft and collinear singularities. These can be separated from the hard phase-space regions by introducing a cutoff parameter $s_{\rm min}$ [18–22]. The hard part can be integrated numerically, whereas the soft or collinear part is treated analytically. The analytical integrals can be performed in $n=4-2\epsilon$ dimensions. The poles which appear in ϵ cancel against poles from the one-loop corrections. Remaining poles in the initial state are proportional to the Altarelli-Parisi splitting functions and are absorbed into the parton distribution functions (PDF's) of the proton, $f_i(x,\mu_F)$ for $i=q,\bar{q},g$. UV divergencies in the one-loop corrections are absorbed into the running coupling constant $\alpha_s(\mu_R)$.

The $\mathcal{O}(\alpha_s)$ corrections to the $\mathcal{O}(\alpha_s^0)$ Born term are known for quite some time [24] and the one-jet inclusive final states have been discussed in [21,25]. Since we will later on rely on programs provided together with the MEPJET Monte Carlo program [26] for tabulating the integrals that occur for the initial state corrections, we will here apply the method of crossing functions as used in [26] and outlined in [27], which is fully equivalent to the results in [21,25]. We take over the notation in [27]. The finite part of the NLO partonic cross section, which is arrived at by summing up the virtual contributions and the singular parts of the two-parton final state is given by the expression

$$\alpha_s \hat{\sigma}^{\rm NLO}_{q\to q} = \alpha_s \sigma_0 e_q^2 |M_{q\to q}|^2 \mathcal{K}_{q\to q}(s_{\rm min}, Q^2). \tag{22}$$

The finite parts of the virtual corrections factorize the Born matrix element. The factor $\mathcal{K}_{q\to q}$, depending on both $s_{\rm min}$ and the invariant mass of the hard partons $2p_0\cdot p_1 = Q^2$, is given by

$$\mathcal{K}_{q\to q}(s_{\rm min}, Q^2) = \frac{8}{9}\left(\frac{N_C}{2\pi}\right)\left[-\ln^2\left(\frac{s_{\rm min}}{Q^2}\right) - \frac{3}{2}\ln\left(\frac{s_{\rm min}}{Q^2}\right) - \frac{\pi^2}{3} - \frac{1}{2} + \mathcal{O}(s_{\rm min})\right], \tag{23}$$

where $N_C = 3$ is the number of colors. $\mathcal{K}_{q\to q}$ may be crossed in exactly the same manner as the usual tree level crossing from the $\mathcal{K}$ factor in $e^+e^- \to 2$ partons as given in Eq. (4.31) with $n=0$ in Ref. [20] or in Eq. (3.1.68) of [22]. Thus, Eq. (23) includes also the crossing of a pair of collinear partons with an invariant mass smaller than $s_{\rm min}$ from the final state to the initial state. This ''wrong'' contribution is replaced by the correct collinear initial state configuration by adding the appropriate crossing function contribution to the hadronic cross section, which also takes into account the corresponding factorization of the initial state singularities, encoded in the crossing functions $C_q^{\overline{\rm MS}}$ for valence and sea quark distributions. The crossing functions for an initial state parton a, which participates in the hard scattering process, can be written in the form [27]

$$C_a^{\overline{\rm MS}}(x,\mu_F,s_{\rm min}) = \left(\frac{N_C}{2\pi}\right)\left[A_a(x,\mu_F)\ln\left(\frac{s_{\rm min}}{\mu_F^2}\right) + B_a^{\overline{\rm MS}}(x,\mu_F)\right], \tag{24}$$

with

$$A_a(x,\mu_F) = \sum_p A_{p\to a}(x,\mu_F), \tag{25}$$

and

$$B_a^{\overline{\rm MS}}(x,\mu_F) = \sum_p B_{p\to a}^{\overline{\rm MS}}(x,\mu_F). \tag{26}$$

The sum runs over $p = q, \overline{q}, g$. The individual functions $A_{p\to a}(x,\mu_F)$ and $B_{p\to a}^{\overline{\rm MS}}(x,\mu_F)$ are stated in the Appendix. In particular all plus prescriptions associated with the factorization of the initial state collinear divergencies are absorbed in the crossing functions $C_q^{\overline{\rm MS}}$ which is very useful for a Monte Carlo approach. We note that although the two-parton final state contributions (20) and (21) contain the full polarization dependence of the virtual photon, the singular contributions occur only for the transverse photon polarization.

Taking into account now virtual, initial, and final state corrections we can write the hadronic cross section for the one-parton final state up to $\mathcal{O}(\alpha_s)$ as

$$\sigma_{\rm had}^{\rm 1parton}(s_{\rm min}) = \sigma_0 \sum_{i=q,q}{}_{-} e_i^2 \int dx\, d{\rm PS}^{(k'+1)} \{ f_i(x,\mu_F) \times [1+\alpha_s(\mu_R)\mathcal{K}_{q\to q}(s_{\rm min},Q^2)] + \alpha_s(\mu_R) C_i^{\overline{\rm MS}}(x,\mu_F,s_{\rm min})\} |M_{q\to q}|^2. \tag{27}$$

To obtain the final, $s_{\rm min}$ independent result, one also has to add the contribution containing the two parton final state, integrated over those phase-space regions where any pair of partons i,j with $s_{ij} = (p_i + p_j)^2$ has $s_{ij} > s_{\rm min}$:

$$\sigma_{\rm had}^{\rm 2parton}(s_{\rm min}) = \sigma_0 \sum_{i=q,q}{}_{-} e_i^2 \int_{|s_{ij}|>s_{\rm min}} dx\, d{\rm PS}^{(k'+2)} 4\pi\alpha_s(\mu_R) \times [f_i(x,\mu_F)|M_{q\to qg}|^2 + \tfrac{1}{2} f_g(x,\mu_F)|M_{g\to q\overline{q}}|^2]. \tag{28}$$

The Lorentz-invariant phase space measure $d{\rm PS}^{(k'+n)}$ contains both the scattered electron and the partons from the photon-parton scattering process and is defined as

$$d{\rm PS}^{(k'+n)} = \delta^4\left(p_0 + k - k' - \sum_{i=1}^n p_i\right) 2\pi \frac{d^3k'}{2E'} \prod_{i=1}^n \frac{d^3p_i}{(2\pi)^3 2E_i}. \tag{29}$$

The bremsstrahlung contribution in Eq. (28) grows with $\ln^2 s_{\rm min}$ and $\ln s_{\rm min}$ with decreasing $s_{\rm min}$. Once $s_{\rm min}$ is small enough for the soft and collinear approximations to be valid, this logarithmic growth is exactly canceled by the explicit $-\ln^2 s_{\rm min}$ and $-\ln s_{\rm min}$ terms in $\mathcal{K}_{q\to q}$ and the $s_{\rm min}$ dependence in the crossing functions.

B. Cutoff function

We are now in the position to reformulate the PSS method for the single-jet inclusive cross section for our purposes. As explained in Sec. II, we wish to avoid the NLO one-parton contributions contained in Eq. (27) completely. Integrating out the delta function (29) in Eq. (27) we obtain, omitting scale dependences,

$$\frac{d\sigma_{\rm had}^{\rm 1parton}}{dx\, dQ^2} = \frac{2\pi\alpha}{xQ^4}[1+(1-y)^2] \sum_{i=q,q}{}_{-} e_i^2 x\{ f_i(x) \times [1+\alpha_s \mathcal{K}_{q\to q}(Q^2)] + \alpha_s C_i^{\overline{\rm MS}}(x)\}. \tag{30}$$

The $s_{\rm min}$ dependence of this one-parton cross section is canceled by the respective unresolved two-parton cross section for each phase-space point (x,Q^2). In order to avoid the one-parton final states, it will be sufficient to chose an appropriate value of the cutoff parameter (which we denote as $s_{\rm min}^{\rm nlo}$) for each phase-space point (x,Q^2), so that

$$\frac{d\sigma_{\rm had}^{\rm 1parton}}{dx\, dQ^2}(s_{\rm min}^{\rm nlo}) = 0. \tag{31}$$

To solve Eq. (31) for $s_{\min}$, it is sufficient to solve the equation

$$\sum_{i=q,q}{}_{-} e_i^2 \{ f_i(x,\mu_F)[1+\alpha_s(\mu_R)\mathcal{K}_{q\to q}(s_{\min},Q^2)] + \alpha_s(\mu_R) C_i^{\overline{\rm MS}}(x,\mu_F,s_{\min})\} = 0. \tag{32}$$

The $s_{\min}$ dependence of $\mathcal{K}_{q\to q}$ can be seen in Eq. (23), whereas the $s_{\min}$ dependence of $C_i^{\overline{\rm MS}}$ is given in Eq. (24). For convenience, we define the sums

$$F = \sum_{i=q,q}{}_{-} e_i^2 f_i(x,\mu_F), \tag{33}$$

$$A = \sum_{i=q,q}{}_{-} e_i^2 A_i(x,\mu_F), \tag{34}$$

$$B = \sum_{i=q,q}{}_{-} e_i^2 B_i^{\overline{\rm MS}}(x,\mu_F) \tag{35}$$

and the functions

$$\eta = \ln\left(\frac{Q^2}{M^2}\right) - \frac{3}{4} + \frac{9}{16}\frac{A}{F}, \tag{36}$$

$$\psi = -\ln^2\left(\frac{Q^2}{M^2}\right) + \frac{3}{2}\ln\left(\frac{Q^2}{M^2}\right) - \frac{\pi^2}{3} - \frac{1}{2} + \frac{9}{8}\left[\frac{2\pi}{N_C\alpha_s} + \frac{B}{F} - \frac{A}{F}\ln\left(\frac{\mu_F^2}{M^2}\right)\right], \tag{37}$$

which are independent of $s_{\min}$ up to $\mathcal{O}(s_{\min})$. We have introduced some arbitrary scale M^2 to keep the functions η and ψ dimensionless. The solution of Eq. (32) is then given by the solution of the quadratic equation

$$\ln^2\left(\frac{s_{\min}}{M^2}\right) - 2\eta\ln\left(\frac{s_{\min}}{M^2}\right) = \psi. \tag{38}$$

We find for $s_{\min}^{\rm nlo}$

$$s_{\min}^{\rm nlo}(\mu_F,\mu_R,x,Q^2) = \exp[\ln(M^2) + \eta - \sqrt{\eta^2+\psi}], \tag{39}$$

where we have taken the smaller of the two solutions, since we require $s_{\min}$ to be sufficiently small for the soft and collinear approximations to be valid. The $\ln(M^2)$ dependence in Eq. (39) cancels in the sum of the individual terms in the exponent.

Inserting the $s_{\min}^{\rm nlo}$ function into Eq. (28) as a lower integration boundary for each phase space point (x,Q^2) will give the complete answer for the single-jet cross section in NLO. This is well suited for the purpose of combining matrix elements in NLO with the PS. It is important to note that the $s_{\min}^{\rm nlo}$ function depends on the factorization and renormalization scales, so that the improved scale dependence of the NLO cross section is preserved in our modified approach. A crucial point, which we will study in detail in the next section, is whether the $s_{\min}^{\rm nlo}$ function obtained with Eq. (39) is small enough for the soft and collinear approximations, made to evaluate the expressions (23) and (24), to be valid.

C. Numerical results

In this section we numerically investigate the solution (39). We look at the size of $s_{\min}^{\rm nlo}$ for given x and Q^2 and study the effect of scale changes on $s_{\min}^{\rm nlo}$. Furthermore, we check whether NLO single-jet inclusive cross sections obtained by integrating out the two-parton contributions down to $s_{\min}^{\rm nlo}$ gives the same result as in the conventional approach, where one-parton and two-parton contributions, separated by some fixed $s_{\min}$, are summed.

We start by looking at the $s_{\min}^{\rm nlo}$ function in the region given by $x\in[10^{-4},10^{-1}]$ and $Q^2\in[10,10^4]$ GeV^2. We produce all results for one-photon exchange, i.e., neglecting possible contributions from Z-exchange. We employ the Martin-Roberts-Stirling-Thorne (MRST) [28] parton distributions for the proton and use the integration package provided with MEPJET to calculate and tabulate the crossing functions [26] for these parton distributions. This makes it numerically very convenient to use the function $s_{\min}^{\rm nlo}$, Eq. (39).[2] In Fig. 1 we have plotted $s_{\min}^{\rm nlo}$ as a function of Q^2 for the four fixed values $x=10^{-4}$, 10^{-3}, 10^{-2}, and 10^{-1} for the scales $\mu=\mu_R=\mu_F=\xi Q^2$ with $\xi=\frac{1}{4}$, 1, and 4. We find values around 2 GeV^2 in the small Q^2 region, whereas they rise up to values between 100 and 200 GeV^2 for the largest Q^2 values. The $s_{\min}$ values are larger for smaller x. The scale variation lead to small changes of the $s_{\min}$ values. The scale variation in the actual cross sections will be still smaller, since the $s_{\min}$ dependence of the cross sections is logarithmic. For the two larger x values, the smaller scales leads to a larger value of $s_{\min}^{\rm nlo}$ which will therefore produce smaller cross sections. For the two smaller x values there seems to be a compensation between the renormalization and factorization scale variations, leading to a very small overall variation in $s_{\min}^{\rm nlo}$, especially at large Q^2.

Next, we numerically compare the standard PSS method with our modified approach. The following comparisons are done for HERA conditions, i.e., $E_e=27.5$ GeV and $E_p=820$ GeV, giving $\sqrt{s}=300$ GeV. A cut of $E_e'>10$ GeV is applied to the final state electron and we choose $y\in[0.04,1]$. We take the same Q^2 region as above, namely, $Q^2\in[10,10^4]$ GeV^2. Jets are defined in the laboratory frame with the k_T algorithm with $E_T^{\rm lab}>5$ GeV and $|\eta^{\rm lab}|<2$. All cuts together restrict the x range to be $x\in[10^{-3},1]$. The numerical results for the one-jet inclusive cross sections in the following are produced with MEPJET [26].

In Fig. 2 we plot the NLO cross sections for the one-parton final states, which include the Born term, the virtual corrections, and the soft and collinear contributions, together

[2]The FORTRAN code for the $s_{\min}^{\rm nlo}$ function can be obtained upon request from the author.

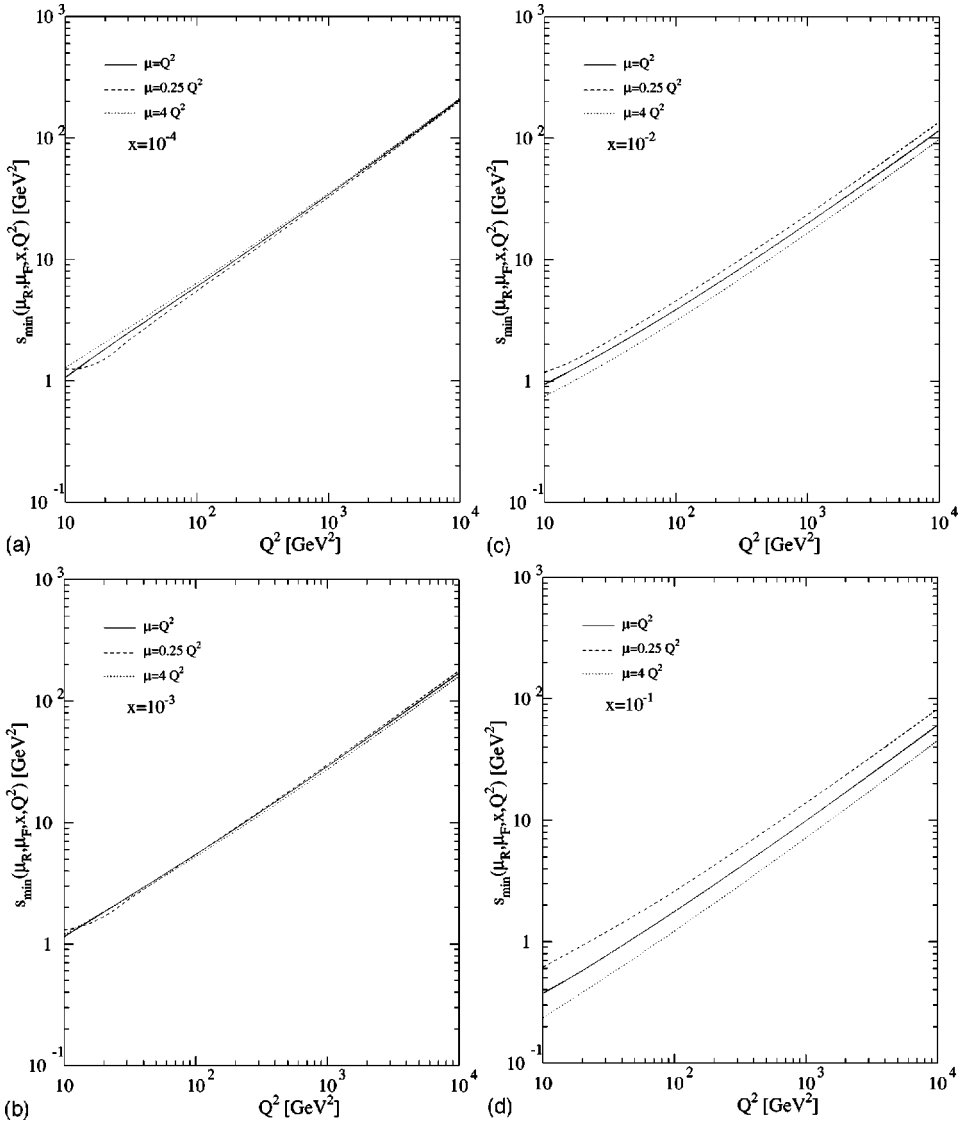

FIG. 1. The function $s_{\min}$ versus Q^2 for the scales $\mu_R=\mu_F=\frac{1}{4}Q^2,Q^2,4Q^2$ for the four values $x=10^{-4}$, 10^{-3}, 10^{-2}, and 10^{-1}.

with the hard two-parton final states and their sum as a function of $s_{\min}$ for four different Q^2 regions integrated over the whole x range. In Fig. 2(a) we see how the logarithmic $s_{\min}$ dependence of the two-parton final states is compensated by the one-parton final states to give an $s_{\min}$ independent result of $\sigma=11.66\pm0.02$ nb up to values of $s_{\min}\simeq10$ GeV^2. Above that value a slight variation of the sum can be observed and the $s_{\min}$ independence is no longer ensured. For $s_{\min}>30$ GeV^2 the one-parton final state obviously fails to give a correct $s_{\min}$ dependence and the sum of one- and two-parton final states strongly decreases. We note that at even larger $s_{\min}$ values, the one-parton final states will again give zero, which is the second solution of Eq. (32) which we rejected in Eq. (39). As an important result, one also sees that the value of $s_{\min}$, for which the one-parton final states vanish and the two-parton final states give the full answer is well within the $s_{\min}$ independent region. Indeed, after we have introduced our $s_{\min}^{\rm nlo}$ function into the MEPJET program we found that the one-parton final states did give zero and as a result for the two-parton final state we found $\sigma=11.59\pm0.01$ nb, which agrees with the answer for small $s_{\min}$ very well. Similar results hold for the larger Q^2 ranges, Figs. 2(b)–2(d). The point at which the NLO one-parton final state contributions vanish are well within the $s_{\min}$ independent region. This holds also for the largest Q^2 values, where the absolute size of the $s_{\min}$ function is rather large, of the order of 100 GeV^2, as we have seen in Fig. 1. At the largest Q^2 values the results seem to become even more stable with respect to the $s_{\min}$ dependence.

For a more detailed study we have calculated the single-jet inclusive cross section for nine different bins in x and Q^2, namely, $Q^2\in[10,10^2]$ GeV^2, $Q^2\in[10^2,10^3]$ GeV^2, and $Q^2\in[10^3,10^4]$ GeV^2 together with $x\in[10^{-3},10^{-2}]$, $x\in[10^{-2},0.1]$, and finally $x\in[0.1,1]$. The actual bins are summarized in Table I. In addition, we have tested the scale dependence by varying the squared renormalization and factorization scales together by a factor of 4, i.e., $\mu^2=\mu_R^2=\mu_F^2=\xi Q^2$ with $\xi=\frac{1}{4},1,4$. The results are shown in Tables II–IV in pb, also indicating the relative difference $\Delta=|\sigma_{\rm std}-\sigma_{\rm mod}|/\sigma_{\rm std}$ of the standard PSS method to the modified PSS. For all Q^2 intervals we find agreement of our modified approach compared to the $s_{\min}$ independent standard ap-

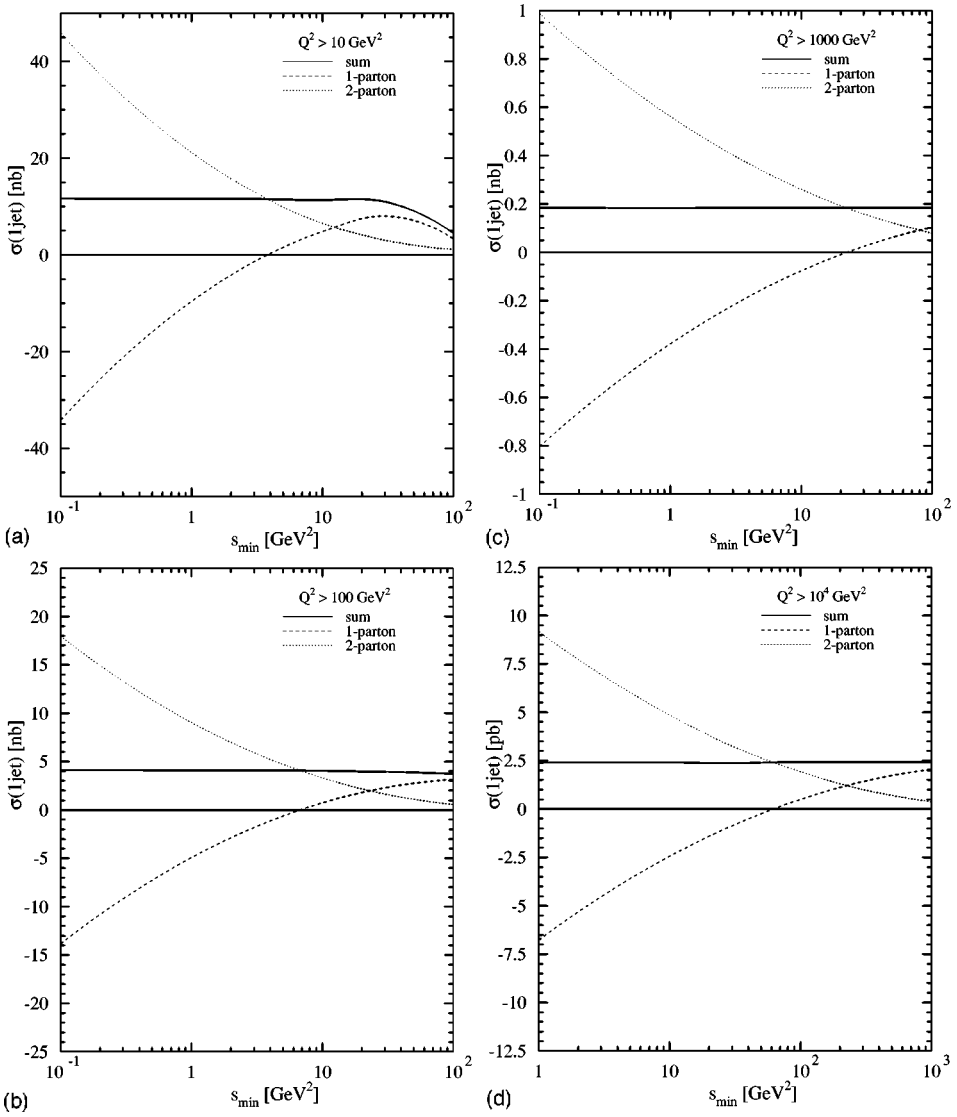

FIG. 2. Inclusive single-jet cross section for $E_T^{\rm lab}>5$ GeV, $|\eta^{\rm lab}|<2$, and $Q^2>10$ GeV^2 as a function of $s_{\rm min}$. The $s_{\rm min}$ values at which the one-parton contributions vanish lie well within the $s_{\rm min}$ independent region for all Q^2.

proach to around 1% or better. The overall scale dependence is small, indicating a very good perturbative stability, as to be expected. However, it was not our intention to test the scale dependence, but to test whether our $s_{\rm min}^{\rm nlo}$ function would reproduce the scale behavior correctly.

This concludes our numerical studies, showing the equivalence of the standard PSS method with our modified approach by integrating out only the two-parton final states down to a dynamical $s_{\rm min}^{\rm nlo}$ function given by Eq. (39).

IV. SUMMARY AND OUTLOOK

We have given a prescription for combining fixed NLO matrix elements with PS's within the PSS method. It consists in removing the Born, virtual, and soft or collinear contributions from the NLO cross section for the n-jet region by adjusting the PSS parameter $s_{\rm min}$ for each phase space point and each scale μ_R,μ_F. These contributions are then included in the hard part of the NLO matrix elements, which

TABLE I. Bins in x and Q^2 (given in GeV^2) for $y>0.04$. Two bins are kinematically excluded.

	$Q^2\in[10,10^2]$	$Q^2\in[10^2,10^3]$	$Q^2\in[10^3,10^4]$
$x\in[10^{-1},1]$		bin 3	bin 6
$x\in[10^{-1},10^{-2}]$	bin 1	bin 4	bin 7
$x\in[10^{-2},10^{-3}]$	bin 2	bin 5	

TABLE II. Cross sections in pb for the bins 1–7 defined in Table I, comparing the standard PSS method with the $s_{\rm min}^{\rm nlo}$ modified PSS method for three different scales. Δ gives the difference of both methods in percent.

	Scale $\mu^2=Q^2$		
Bin	Standard PSS	modified PSS	Δ
1	1044 ± 3	1037 ± 2	0.7
2	5734 ± 15	5700 ± 9	0.6
3	19.99 ± 0.18	20.22 ± 0.04	1.2
4	2193 ± 3	2214 ± 4	1.0
5	1882 ± 4	1875 ± 2	0.4
6	54.10 ± 0.20	55.60 ± 0.18	2.8
7	129.3 ± 0.5	131.1 ± 0.4	1.4

TABLE III. Same as Table II for $\mu^2=4Q^2$.

Scale $\mu^2=4Q^2$			
Bin	Standard PSS	Modified PSS	Δ
1	1124 ± 4	1120 ± 2	0.4
2	6218 ± 15	6191 ± 7	0.4
3	19.97 ± 0.18	20.15 ± 0.04	1.0
4	2260 ± 4	2288 ± 5	1.2
5	1987 ± 6	1981 ± 2	0.3
6	54.21 ± 0.22	55.69 ± 0.13	2.7
7	130.9 ± 0.8	132.1 ± 0.2	1.0

are positive definite. This allows to directly redistribute the weight provided from these matrix elements with a PS algorithm.

For the case of inclusive single-jet production in eP scattering at $\mathcal{O}(\alpha_s)$ we have calculated the dynamical $s_{\min}$ parameter for each phase space point x and Q^2 and each scale μ_R, μ_F. We have numerically compared the standard calculation with our new approach of evaluating fixed NLO contributions and found the new approach to give reliable results. We especially found that the values of $s_{\min}$, for which the virtual plus soft or collinear contributions vanish, are small enough for the soft and collinear approximations, used in the PSS method, to be valid. We note that the cutoff function has been successfully implemented in the RAPGAP event generator [29], which includes the $\mathcal{O}(\alpha_s)$ tree level matrix elements. Numerical results and comparison to data will be discussed in a forthcoming paper.

The next, more complicated step is the case of dijet production in eP scattering, which is especially interesting because it allows a precise determination of α_s or the gluon density in the proton. NLO calculations in the PSS method from which the cutoff function can be determined are available [21,26,27,30]. It might turn out that the PSS method has to be supplemented with the hybrid method to numerically evaluate terms of order $s_{\min}\ln(s_{\min})$ as outlined in Sec. II. NLO calculations within the subtraction method are available for dijet production in eP scattering [17], so that the expressions needed for the hybrid of PSS and subtraction method can readily be evaluated. We finally note that the $\mathcal{O}(\alpha_s^2)$ tree level matrix elements for eP scattering interfaced with the PS are not yet available in a working Monte Carlo event generator.

TABLE IV. Same as Table II for $\mu^2=\frac{1}{4}Q^2$.

Scale $\mu^2=\frac{1}{4}Q^2$			
Bin	Standard PSS	Modified PSS	Δ
1	984.1 ± 3	970.7 ± 2	1.4
2	5412 ± 14	5343 ± 6	1.3
3	20.00 ± 0.21	20.30 ± 0.05	1.5
4	2134 ± 5	2158 ± 6	1.1
5	1781 ± 6	1758 ± 2	1.3
6	54.90 ± 0.29	55.90 ± 0.21	1.8
7	129.0 ± 0.9	130.3 ± 0.3	1.0

ACKNOWLEDGMENTS

We have benefited from discussions with S. Catani, H. Jung, G. Kramer, J. Rathsman, T. Schörner, T. Sjöstrand, and M. Sutton. I am grateful to G. Kramer for comments on the manuscript. D. Chapin and N. Kauer have been helpful concerning details of the MEPJET program.

APPENDIX: CROSSING FUNCTIONS

For reasons of completeness, in this appendix we collect from [27] the definitions of the functions $A_{p\to a}$ and $B^{\overline{\rm MS}}_{p\to a}$ which are needed to compute the crossing functions $C_i^{\overline{\rm MS}}$. The functions are defined via a one dimensional integration over the parton densities f_p, which also involves the integration over $()_+$ prescriptions. The finite, scheme independent functions $A_{p\to a}(x,\mu_F)$ are given by

$$A_{g\to g}=\int_x^1\frac{dz}{z}f_g(x/z,\mu_F)\left\{\frac{(11N_C-2n_f)}{6N_C}\delta(1-z)+2\left(\frac{z}{(1-z)_+}+\frac{(1-z)}{z}+z(1-z)\right)\right\},\tag{A1}$$

$$A_{q\to q}=\int_x^1\frac{dz}{z}f_q(x/z,\mu_F)\frac{2C_F}{3}\left\{\frac{3}{4}\delta(1-z)+\frac{1}{2}\left(\frac{1+z^2}{(1-z)_+}\right)\right\},\tag{A2}$$

$$A_{g\to q}=\int_x^1\frac{dz}{z}f_g(x/z,\mu_F)\frac{1}{4}\hat{P}^{(4)}_{g\to q}(z),\tag{A3}$$

$$A_{q\to g}=\int_x^1\frac{dz}{z}f_q(x/z,\mu_F)\frac{1}{4}\hat{P}^{(4)}_{q\to g}(z).\tag{A4}$$

The scheme dependent functions $B^{\overline{\rm MS}}_{p\to h}(x,\mu_F)$ are given by

$$B^{\overline{\rm MS}}_{g\to g}=\int_x^1\frac{dz}{z}f_g(x/z,\mu_F)\left\{\left(\frac{\pi^2}{3}-\frac{67}{18}+\frac{5n_f}{9N_C}\right)\delta(1-z)+2z\left(\frac{\ln(1-z)}{(1-z)}\right)_+ +2\left(\frac{(1-z)}{z}+z(1-z)\right)\times\ln(1-z)\right\},\tag{A5}$$

$$B^{\overline{\rm MS}}_{q\to q}=\int_x^1\frac{dz}{z}f_q(x/z,\mu_F)\frac{2C_F}{3}\left\{\left(\frac{\pi^2}{6}-\frac{7}{4}\right)\delta(1-z)+\frac{1}{2}(1-z)+\frac{1}{2}(1+z^2)\left(\frac{\ln(1-z)}{(1-z)}\right)_+\right\},\tag{A6}$$

$$B^{\overline{\rm MS}}_{g\to q}=\int_x^1\frac{dz}{z}f_g(x/z,\mu_F)\frac{1}{4}\{\hat{P}^{(4)}_{g\to q}(z)\ln(1-z)-\hat{P}^{(\epsilon)}_{g\to q}(z)\},\tag{A7}$$

$$B^{\overline{\rm MS}}_{q\to g}=\int_x^1\frac{dz}{z}f_q(x/z,\mu_F)\frac{1}{4}\{\hat{P}^{(4)}_{q\to g}(z)\ln(1-z)-\hat{P}^{(\epsilon)}_{q\to g}(z)\}.\tag{A8}$$

Here, n_f denotes the number of flavors and $N_C=3$ is the number of colors. The Altarelli-Parisi kernels in the previous equations are defined by:

$$\hat{P}^{(n\neq 4)}_{g\to g}(z)=P^{(n\neq 4)}_{g\to g}(z)=4\left(\frac{z}{1-z}+\frac{1-z}{z}+z(1-z)\right),\tag{A9}$$

$$\hat{P}^{(n\neq 4)}_{q\to g}(z)=\frac{8}{9}P^{(n\neq 4)}_{q\to g}(z)=\frac{16}{9}\left(\frac{1+(1-z)^2}{z}-\epsilon z\right),\tag{A10}$$

$$\hat{P}^{(n\neq 4)}_{g\to q}(z)=\frac{1}{3}P^{(n\neq 4)}_{g\to q}(z)=\frac{2}{3}\left(\frac{z^2+(1-z)^2-\epsilon}{1-\epsilon}\right),\tag{A11}$$

$$\hat{P}^{(n\neq 4)}_{q\to q}(z)=\frac{8}{9}P^{(n\neq 4)}_{q\to q}(z)=\frac{16}{9}\left(\frac{1+z^2}{1-z}-\epsilon(1-z)\right).\tag{A12}$$

The $P^{(\epsilon)}_{ij}$ are the ϵ dimensional part of these n-dimensional splitting functions

$$\hat{P}^{(\epsilon)}_{q\to g}(z)=\frac{8}{9}P^{(\epsilon)}_{q\to g}(z)=-\frac{8}{9}2z,\tag{A13}$$

$$\hat{P}^{(\epsilon)}_{g\to q}(z)=\frac{1}{3}P^{(\epsilon)}_{g\to q}(z)=-\frac{4}{3}z(1-z).\tag{A14}$$

The $()_+$ prescriptions in these equations are defined for an arbitrary test function $G(z)$ (which is well behaved at $z=1$) as

$$\int_x^1 dzF_+(z)G(z)=\int_x^1 dzF(z)[G(z)-G(1)]+G(1)\int_0^x dzF(z).\tag{A15}$$

The structure and use of the crossing functions are completely analogous to the usual parton distribution function.

The numerical integrations have been performed in a computer program, which is provided together with the fixed order Monte Carlo program MEPJET [26]. The results for $A_{p\to a}$ and $B^{\overline{\rm MS}}_{p\to a}$ for different values of x and μ_F are stored in an array in complete analogy to the usual parton densities, which allows a convenient and numerically quick evaluation of the crossing functions.

[1] M. Kuhlen, *QCD at HERA: The Hadronic Final State in Deep Inelastic Scattering* (Springer-Verlag, Berlin, 1999).

[2] *Proceedings of the DESY Workshop on Monte Carlo Generators for HERA Physics*, edited by A. T. Doyle, G. Grindhammer, G. Ingelman, and H. Jung (DESY, Hamburg, 1999).

[3] H1 Collaboration, C. Adloff *et al.*, Eur. Phys. J. C **5**, 625 (1998).

[4] B. Andersson, G. Gustafson, G. Ingelman, and T. Sjöstrand, Phys. Rep. **97**, 31 (1983).

[5] M. H. Seymour, Comput. Phys. Commun. **90**, 95 (1995).

[6] G. Corcella and M. H. Seymour, Phys. Lett. B **442**, 417 (1998); Nucl. Phys. **B565**, 227 (2000).

[7] G. Ingelman, A. Edin, and J. Rathsman, Comput. Phys. Commun. **101**, 108 (1997).

[8] M. Bengston and T. Sjöstrand, Phys. Lett. B **185**, 435 (1987); Nucl. Phys. **B289**, 810 (1987); J. André and T. Sjöstrand, Phys. Rev. D **57**, 5767 (1998); G. Miu and T. Sjöstrand, Phys. Lett. B **449**, 313 (1999).

[9] T. Sjöstrand, Comput. Phys. Commun. **82**, 74 (1994).

[10] G. Marchesini *et al.*, Comput. Phys. Commun. **67**, 465 (1992).

[11] S. Mrenna, Report UCD-99-4, hep-ph/9902471.

[12] J. Collins, J. High Energy Phys. **05**, 4 (2000).

[13] C. Friberg and T. Sjöstrand, in *Proceedings of the DESY Workshop on Monte Carlo Generators for HERA Physics* [2], hep-ph/9906316.

[14] H. Baer and M. H. Reno, Phys. Rev. D **44**, R3375 (1991); **45**, 1503 (1992); **54**, 2017 (1996).

[15] R. K. Ellis, D. A. Ross, and A. E. Terrano, Nucl. Phys. **B178**, 421 (1981).

[16] Z. Kunszt and D. E. Soper, Phys. Rev. D **46**, 192 (1992).

[17] S. Catani and M. H. Seymour, Phys. Lett. B **378**, 287 (1996); Nucl. Phys. **B485**, 291 (1997).

[18] K. Fabricius, G. Kramer, G. Schierholz, and I. Schmitt, Z. Phys. C **11**, 315 (1982); F. Gutbrod, G. Kramer, G. Rudolph, and G. Schierholz, *ibid.* **35**, 543 (1987).

[19] H. Baer, J. Ohnemus, and J. F. Owens, Phys. Rev. D **40**, 2844 (1989); **42**, 61 (1990); Phys. Lett. B **234**, 127 (1990).

[20] W. T. Giele and E. W. N. Glover, Phys. Rev. D **46**, 1980 (1992).

[21] D. Graudenz, Phys. Rev. D **49**, 3291 (1994); Phys. Lett. B **256**, 518 (1992).

[22] G. Kramer, *Theory of Jets in Electron-Positron Annihilation* (Springer-Verlag, Berlin, 1984).

[23] E. W. N. Glover and M. R. Sutton, Phys. Lett. B **342**, 375 (1995).

[24] G. Altarelli, R. K. Ellis, and G. Martinelli, Nucl. Phys. **B143**, 521 (1978); **B146**, 544(E) (1978); **B157**, 461 (1979); A. Mendez, *ibid.* **B145**, 199 (1978); A. Mendez and T. Weiler, Phys. Lett. **83B**, 221 (1979); R. D. Peccei and R. Rückl, Nucl. Phys. **B162**, 125 (1980); Ch. Rumpf, G. Kramer, and J. Willrodt, Z. Phys. C **7**, 337 (1981).

[25] J. G. Körner, E. Mirkes, and G. A. Schuler, Int. J. Mod. Phys. A **4**, 1781 (1989).
[26] E. Mirkes and D. Zeppenfeld, Phys. Lett. B **380**, 23 (1996); Acta Phys. Pol. B **27**, 1392 (1996).
[27] E. Mirkes, Habilitationsschrift 1997, TTP97-39, hep-ph/9711224.
[28] A. D. Martin, R. G. Roberts, W. J. Stirling, and R. S. Thorne, Eur. Phys. J. C **4**, 463 (1998).
[29] H. Jung, Comput. Phys. Commun. **86**, 147 (1995).
[30] G. Kramer and B. Pötter, Eur. Phys. J. C **5**, 665 (1998); B. Pötter, Eur. Phys. J. Direct **C5**, 1 (1999).